Journal of Materials Chemistry C

PAPER

View Article Online
View Journal | View Issue

Cite this: J. Mater. Chem. C, 2018, 6, 13331

An easy-to-make strong white AIE supramolecular polymer as a colour tunable photoluminescence material†

Yan-Qing Fan,[a] Juan Liu,*[b] Yan-Yan Chen,[a] Xiao-Wen Guan,[a] Jiao Wang,[a] Hong Yao,[a] You-Ming Zhang,[a] Tai-Bao Wei*[a] and Qi Lin*[a]

Received 7th September 2018,
Accepted 15th November 2018

DOI: 10.1039/c8tc04540b

rsc.li/materials-c

An easy-to-make supramolecular polymer was successfully constructed by self-assembly of tripodal tri-(pyridine-4-yl)-functionalized trimesic amide (**DTB**) in DMSO–H_2O binary solutions. The supramolecular polymer **DTB** showed strong white aggregation-induced emission (AIE) in the solid state as well as in water suspensions. **DTB** could also form a stable supramolecular polymer hydrogel (**DTB-G**) in pure water. Interestingly, **DTB** showed excellent coordination ability for rare earth metal ions (Tb^{3+}, Eu^{3+}, La^{3+}, Th^{4+} and Ce^{3+}) and formed the corresponding complexes (**DTB-Ms**). Interestingly, by introducing the above-mentioned rare earth metal ions, the fluorescence colour of the obtained **DTB-Ms** showed corresponding variations. By inseting UV-LED lamps (λ = 365 nm) into different rare earth metal ion-coordinated xerogel **DTB-Ms** in small test tubes, a series of LED devices with multicolour lights were obtained. Therefore, **DTB** and **DTB-Ms** can act as fluorescence colour-tunable photoluminescence materials.

Introduction

In recent years, multicolour photoluminescence materials[1] have attracted significant research interest due to their extensive applications in lighting devices and display media,[2] optical sensors[3] and switches.[4] In the quest for white-light emitting materials,[5] supramolecular systems[6] displaying different stimuli-responsive emission colours are attracting considerable attention. Meanwhile, white light-emissive materials have also attracted increasing attention owing to their potential application in lighting devices and display media.[7] As white-light emission covers the whole visible region from 400 to 700 nm, the generation of white-light emission commonly requires simultaneous emission of three primary RGB colours (red, green and blue) or at least two complementary colours.[8] However, serious problems are encountered such as spectral instability and bad colour reproducibility.[9] To date, the most common strategy to solve these problems is to develop small-molecule luminophores to emit white light efficiently in the solid state. In recent years, a variety of approaches have been reported to develop efficient white-light emission systems such as polymers,[10] metal organic frameworks,[11] and small molecules.[12] However, it is still a challenge to develop small-molecule luminophores that emit white light in the solid state.

The rare-earth metal ions Tb^{3+}, Eu^{3+}, La^{3+}, Ce^{3+} and Th^{4+} play pivotal roles in many fields such as medical diagnostics, optical imaging,[13] and luminescent sensing.[14] Due to their excellent coordination ability and fluorescence properties, they are used by many scientists. A series of rare earth metal ions have been applied as photoluminescence materials.[15] However, as a heavy metal ion waste, these ions may lead to long-term potential threat to soils, groundwater and human beings;[16] thus, the detection and separation of these rare-earth metal ions are very important.

In view of these observations and as a part of our research interest in supramolecular functional materials,[17,18] herein, we reported a simple supramolecular polymer that was self-assembled from an easy-to-make tripodal gelator tri-(pyridine-4-yl)-functionalized trimesic amide (**DTB**). **DTB** could form a supramolecular polymer hydrogel (**DTB-G**) in water and showed strong white aggregation-induced emission (AIE). Interestingly, **DTB** showed excellent coordination ability for rare earth metal ions (Tb^{3+}, Eu^{3+}, La^{3+}, Th^{4+} and Ce^{3+}) and formed corresponding complexes (**DTB-Ms**). Also, by introducing the above-mentioned rare earth metal ions, the fluorescence colour of the obtained **DTB-Ms** showed corresponding variation. Therefore, **DTB** could act as a fluorescence colour-tunable photoluminescence material. Moreover, by coordination with Tb^{3+}, Eu^{3+}, La^3 and Ce^{3+}, **DTB** could

[a] Key Laboratory of Polymer Materials of Gansu Province, College of Chemistry and Chemical Engineering, Northwest Normal University, Lanzhou 730070, China. E-mail: linqi2004@126.com, weitaibao@126.com

[b] College of Chemical Engineering, Northwest University for Nationalities, Lanzhou 730070, China. E-mail: liujuan656@126.com

† Electronic supplementary information (ESI) available: Experiment details, synthesis of **DTB**, ^1H NMR, ^{13}C NMR and MS spectra, other materials. See DOI: 10.1039/c8tc04540b

form stable supramolecular polymer metallo-hydrogels in pure water. Meanwhile, **DTB** also showed excellent separation properties for Tb^{3+}, Eu^{3+}, La^{3+} and Ce^{3+}.

Results and discussion

As shown in Scheme S1 (ESI†), tripodal **DTB** was first synthesized by a simple one-step reaction between trimesoyl chloride and 4-aminopyridine. **DTB** was dissolved in DMSO (1×10^{-3} M); however, with an increasing amount of pure water in the **DTB**–DMSO solution, the solution showed strong white emission (Fig. 2). As shown in Fig. 1c, a dilute DMSO solution of **DTB** exhibited no Tyndall effect. However, with the addition of water into the dilute solution of **DTB**, a clear Tyndall effect could be observed. Moreover, in the SEM image (Fig. 1 and Fig. S12, ESI†), the **DTB** xerogel obtained from DMSO–H_2O binary solution showed a fibriform structure. These results indicated that with the addition of H_2O in the **DTB**–DMSO solution, **DTB** underwent a self-assembly process, forming a stable fibriform supramolecular polymer. The self-assembly process induced strong white emission. Therefore, the white light emission is an aggregation-induced emission (AIE). Interestingly, **DTB** could form a stable supramolecular hydrogel (c = 1 M) (Fig. 1a). The **DTB** hydrogel (Fig. 1a) and **DTB** xerogel (Fig. 3a) also showed strong white emission. Moreover, the water solubility of **DTB** is very poor. **DTB** was almost insoluble in water. Therefore, in this study, **DTB** was suspended in water, and we carried out the corresponding research by using **DTB** suspensions.

The possible assembly mechanism (Fig. 1) of **DTB** was investigated by fluorescence spectroscopy, IR, XRD, SEM and

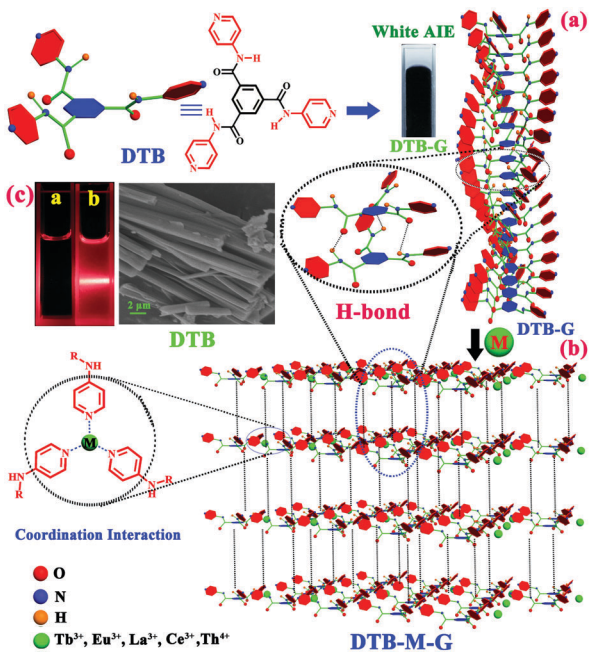

Fig. 1 (a) The photograph of **DTB** hydrogel in water (1 M) and proposed self-assembly mechanism of **DTB**. (b) Proposed coordination mechanism of **DTB** with rare earth metals. (c) Photos showing the Tyndall effect of **DTB** (a: in DMSO; b: in a binary solution of DMSO and H_2O).

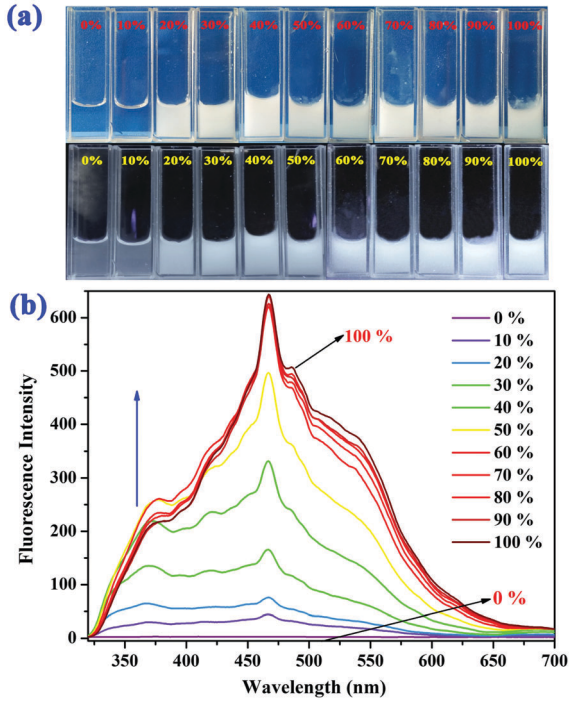

Fig. 2 (a) Photographs of **DTB** solutions containing different water contents. (b) Fluorescence spectra of **DTB** solutions containing different water contents.

concentration-dependent ^{1}H NMR. As shown in Fig. 2, with the addition of water, aggregation-induced emission including white-light emission was observed, and great fluorescence increase was observed at 475 nm after addition of water into the **DTB**–DMSO solution. This result indicated that **DTB** could self-assemble in water. The self-assembly mechanism was also investigated by concentration-dependent ^{1}H NMR (Fig. 3). In the concentration-dependent ^{1}H NMR spectra of **DTB**, with increasing concentration of **DTB**, the proton signals of H^1 (11.27 ppm) and H^2 (8.86 ppm) on **DTB** showed downfield shifts. This indicated that hydrogen bonds existed in the self-assembly process of **DTB**. In addition, in the powder X-ray diffraction (PXRD) pattern of **DTB** xerogel (Fig. S9, ESI†), there are many sharp peaks at 2θ from 15 to 30 degrees, indicating that **DTB** has a long-range ordered structure in the xerogel. Meanwhile, as shown in Fig. 1 and Fig. S12 (ESI†), the

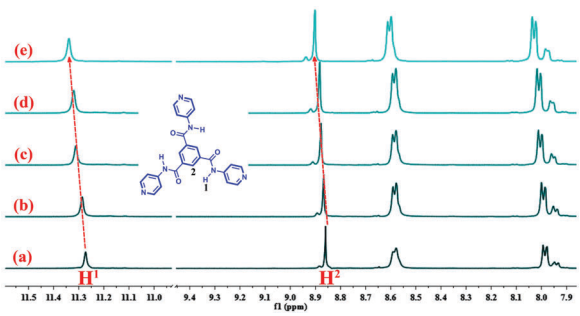

Fig. 3 Partial concentration-dependent ^{1}H NMR spectra of the mixture of **DTB** in DMSO-d_6: (a) 1.37×10^{-2} M; (b) 1.82×10^{-2} M; (c) 2.28×10^{-2} M; (d) 2.73×10^{-2} M; (e) 3.18×10^{-2} M.

morphology of **DTB**, investigated by a scanning electron microscope (SEM), is an orderly fibriform structure. These results indicated that **DTB** could self-assemble to form a supramolecular polymer with an orderly fibriform structure by hydrogen bonds (Fig. 1a).

Then, we introduced rare earth metal ions into water suspensions of **DTB** to investigate the photoluminescence tunable properties of **DTB**. Interestingly, upon the addition of 1.0 equiv. of Tb^{3+}, Eu^{3+}, La^{3+}, Ce^{3+} and Th^{4+} into the water suspension of **DTB** (2.2×10^{-6} M), through coordination with rare earth metal ions, **DTB** could assemble into supramolecular metallo-hydrogels (**DTB-Ms**) with Tb^{3+}, Eu^{3+}, La^{3+} and Ce^{3+} in pure water (Fig. S5, ESI†). More interestingly, the critical gelation concentration (CGC) was lower than 2.2×10^{-6} M [about 0.5% (10 mg mL^{-1} = 1%)], whereas the gel–sol transition temperature (T_{gel}) was in the range from 51.3 to 76.1 °C (Table S1, ESI†). However, with the addition of Th^{4+} into the water suspension of **DTB**, the suspension changed into a clear colourless water solution (Fig. S5, ESI†) and did not form a metallogel.

Interestingly, by introducing rare earth metal ions into **DTB**, the xerogel of **DTB-Ms** showed multicolour tunable photoluminescence properties. As shown in Fig. 4a and 5, compared with the strong white fluorescence emission of **DTB** xerogel, due to the coordination with rare earth metal ions, the fluorescence emission of solid powder or xerogel of **DTB-Ms** changed from white to multicolour photoluminescence. In addition, as shown in Table 1, the xerogel of **DTB** and **DTB-Ms** (**DTB-Tb**, **DTB-Eu**, **DTB-La** and **DTB-Th**) and solid powder of **DTB-Th** with different colour fluorescence emissions have higher fluorescence quantum yields.

Due to the excellent optical properties of rare earth metal ion-coordinated **DTB-Ms**, the applications were primarily investigated. As shown in Fig. 4b, by inseting UV-LED lamps (λ = 365 nm) into the different rare earth metal ion-coordinated xerogels or solid powders of **DTB-Ms** in small test tubes and upon illumination, these xerogels or solid powders emitted bright multicolour lights such as white, red and green. Thus, a series of LED devices with multicolour lights were obtained. Therefore, **DTB** and **DTB-Ms** xerogels or solid powder have potential applications as multicolour photoluminescence materials.

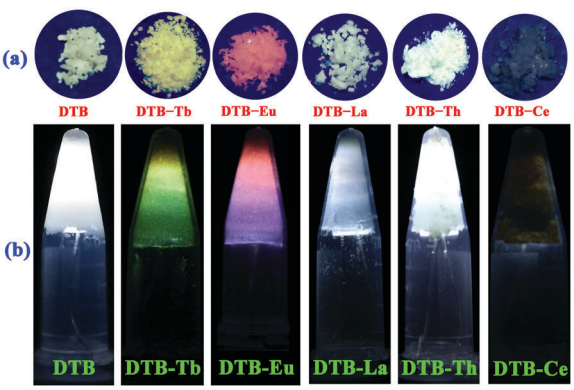

Fig. 4 (a) Fluorescence photographs of xerogel based on rare earth metal ions. (b) Photographs of the 365 nm ultraviolet LED coated with the xerogel of **DTB** and series of **DTB-Ms** (for xerogel, **Ms** is Tb^{3+}, Eu^{3+}, La^{3+} and Ce^{3+}; **DTB-Th** is solid powder of **DTB-Th** complex) when the LED is turned on.

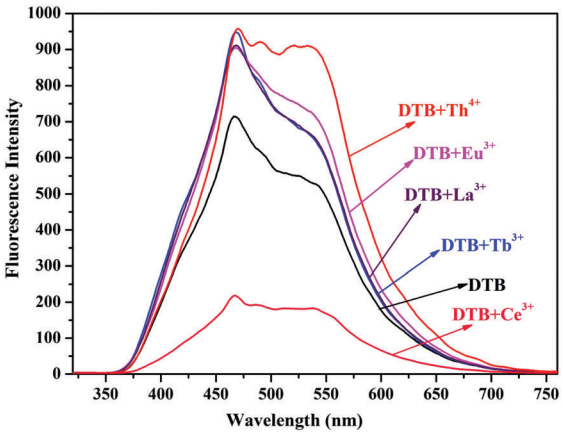

Fig. 5 Fluorescence spectra of xerogel and solid powder of **DTB** and **DTB-M** (for xerogel, **Ms** are Tb^{3+}, Eu^{3+}, La^{3+} and Ce^{3+}; **DTB-Th** is solid powder of **DTB-Th** complex).

Table 1 The fluorescence quantum yields (Y_S) of xerogel **DTB** and **DTB-Ms** (for xerogel, **Ms** are Tb^{3+}, Eu^{3+}, La^{3+} and Ce^{3+}; **DTB-Th** is the solid powder of the **DTB-Th** complex)

State	Samples	Y_S
1	**DTB**	0.452
2	**DTB-Tb**	0.501
3	**DTB-Eu**	0.483
4	**DTB-Th**	0.595
5	**DTB-La**	0.492
6	**DTB-Ce**	0.100

In addition, in view of excellent coordination ability of rare earth metal ions with **DTB** and to explore the adsorption ability of **DTB** for Tb^{3+}, Eu^{3+}, La^{3+} and Ce^{3+}, the adsorption capacity of **DTB** for Tb^{3+}, Eu^{3+}, La^{3+} and Ce^{3+} in water was assessed by inductively coupled plasma (ICP) analysis. The **DTB** xerogel (1 mg, 1×10^{-7} mol) was suspended in a dilute water solution of Tb^{3+}, Eu^{3+}, La^{3+} and Ce^{3+} (all concentrations are about 1×10^{-5} M in 5.0 mL) and stirred for 10 min. Then, the suspension was centrifuged at 10 000 rpm for 5 min, and the precipitate was removed by filtration. The adsorption percentages of the xerogel **DTB** for the above cations in water were assessed by ICP analysis. As shown in Table 2, after the adsorption of these cations by the xerogel of the host powder **DTB** in water, the residual concentrations of Tb^{3+}, Eu^{3+}, La^{3+} and Ce^{3+} were in the

Table 2 The adsorption percentages of xerogel **DTB** for rare earth metal ions

Ions	C_I (μM)	C_R (μM)	AP%
Tb^{3+}	10	0.0796	99.20
Eu^{3+}	10	0.0658	99.34
La^{3+}	10	0.0978	99.02
Ce^{3+}	10	0.0543	99.46

C_I: initial concentration; C_R: residual concentration; AP: absorbing percentage.

range of 5.43×10^{-8} to 9.78×10^{-8} M, and the adsorption percentages of the host powder **DTB** for the above-mentioned cations were up to 99.02–99.46%. These results indicated that **DTB** has excellent adsorption and separation capacities for Tb^{3+}, Eu^{3+}, La^{3+} and Ce^{3+} in water.

The possible coordination mechanisms of **DTB** with Tb^{3+}, Eu^{3+}, La^{3+} and Ce^{3+} were also investigated by IR, XRD and SEM. The IR information of **DTB** and **DTB-Ms** was examined in the solid state at room temperature to prove the coordination mechanism. As shown in Fig. S6 (ESI†), the C=N vibration absorption peaks of pyridine for **DTB** appeared at 1508 cm^{-1}. However, with the addition of Tb^{3+}, Eu^{3+}, La^{3+} and Ce^{3+} into **DTB**, the C=N vibration absorption peaks shifted to 1515, 1522, 1515 and 1522 cm^{-1}, respectively (Fig. S6–S8, ESI†); this indicated that in the above-mentioned coordination interaction, N on pyridine acts as an electron-donating group and forms stable metal coordination interaction with electron acceptors (Tb^{3+}, Eu^{3+}, La^{3+} and Ce^{3+}) (Fig. 1).

Moreover, the powder X-ray diffraction (PXRD) results (Fig. S9–S11, ESI†) support the proposed coordination mechanism. Taking **DTB-Tb** as an example, as shown in Fig. S9 (ESI†), XRD of **DTB-Tb** xerogel shows peaks around 2θ = 19.63, 22.57, 25.11 and 26.25° (d = 4.52, 3.94, 3.55 and 3.40 Å), which indicates that the xerogel of **DTB-Tb** also exists in a long range ordered structure.

Finally, the morphologies of **DTB-Ms** were investigated by a scanning electron microscope (SEM). SEM also supported the proposed coordination mechanism of **DTB-Ms** (Fig. S13, ESI†). The xerogel of **DTB** clearly appears as an orderly fibriform structure (Fig. S12, ESI†). However, after coordination with rare earth metal ions (Tb^{3+}, Eu^{3+}, La^{3+} and Ce^{3+}) and forming **DTB-Ms**, **DTB-Ms** presents as an agminated structure. The results also indicated that there are strong coordination interactions between **DTB** and rare earth metal ions (Tb^{3+}, Eu^{3+}, La^{3+} and Ce^{3+}).

Conclusions

In summary, we successfully constructed an easy-to-synthesize supramolecular polymer **DTB**. **DTB** shows strong white aggregation-induced emission (AIE). **DTB** also shows excellent coordination ability for rare earth metal ions (Tb^{3+}, Eu^{3+}, La^{3+}, Th^{4+} and Ce^{3+}). Furthermore, by introducing the above-mentioned rare earth metal ions into the **DTB** supramolecular polymer, the obtained **DTB-Ms** can emit various fluorescence colours. By inseting UV-LED lamps (λ = 365 nm) into different rare earth metal ion-coordinated **DTB-Ms** xerogels or solid powders in small test tubes, a series of LED devices with multicolour lights were obtained. Therefore, **DTB** and **DTB-Ms** could act as fluorescence colour-tunable photoluminescence materials. Meanwhile, **DTB** complexes have excellent separation properties for Tb^{3+}, Eu^{3+}, La^{3+} and Ce^{3+}. The adsorption percentages of the xerogels for the above metal ions are in the range from 99.02% to 99.46%. **DTB** could also act as a useful material for efficient separation of rare earth metal ions. **DTB** is an easy-to-make small molecular gelator; this research provides a novel approach for developing white-light-emitting and colour-tunable photoluminescence materials by simple small molecules through self-assembly.

Conflicts of interest

There is no conflict to declare.

Acknowledgements

This work was supported by the National Natural Science Foundation of China (NSFC) (No. 21574104; 21662031; 21661028) and the Program for Changjiang Scholars and Innovative Research Team in University of Ministry of Education of China (No. IRT1177).

Notes and references

1 Q. W. Zhang, D. F. Li, X. Li, P. B. White, J. Mecinović, X. Ma, H. Ågren, R. J. M. Nolte and H. Tian, *J. Am. Chem. Soc.*, 2016, **138**, 13541.
2 (*a*) J. Kido, M. Kimura and K. Nagai, *Science*, 1995, **267**, 1332–1334; (*b*) S. Reineke, F. Lindner, G. Schwartz, N. Seidler, K. Walzer, B. Lüssem and K. Leo, *Nature*, 2009, **459**, 234.
3 (*a*) Z. W. Zhuang, C. D. Peng, G. Y. Zhang, H. M. Yang, J. L. Yin and H. H. Fei, *Angew. Chem., Int. Ed.*, 2017, **56**, 14411; (*b*) L. L. Mao, Y. L. Wu, C. C. Stoumpos, M. R. Wasielewski and M. G. Kanatzidis, *J. Am. Chem. Soc.*, 2017, **139**, 5210; (*c*) D. S. Tu, P. Leong, S. Guo, H. Yan, C. S. Lu and Q. Zhao, *Angew. Chem., Int. Ed.*, 2017, **56**, 11370.
4 O. Kotova, S. Comby, C. Lincheneau and T. Gunnlaugsson, *Chem. Sci.*, 2017, **8**, 3419.
5 H. N. Kim, Z. Guo, W. Zhu, J. Yoon and H. Tian, *Chem. Soc. Rev.*, 2011, **40**, 79.
6 (*a*) S. K. Park, I. Cho, J. Gierschner, J. H. Kim, J. H. Kim, J. E. Kwon, O. K. Kwon, D. R. Whang, J. H. Park, B. K. An and S. Y. Park, *Angew. Chem., Int. Ed.*, 2016, **55**, 203; (*b*) H. Mehdi, W. T. Gong, H. M. Guo, M. Watkinson, H. Ma, A. Wajahat and G. L. Ning, *Chem. – Eur. J.*, 2017, **23**, 13067; (*c*) H. Wang, X. M. Qian, X. P. Li and W. T. Gong, *et al.*, *Nat. Commun.*, 2018, **9**, 1815.
7 (*a*) C. Zhang, L. Yang, J. Zhao, B. H. Liu, M. Y. Han and Z. P. Zhang, *Angew. Chem., Int. Ed.*, 2015, **54**, 11531–11535; (*b*) Y. Xia, S. Y. Chen and X. L. Ni, *ACS Appl. Mater. Interfaces*, 2018, **10**, 13048.
8 D. F. Li, W. D. Hu, J. Wang, Q. W. Zhang, X. M. Cao, X. Ma and H. Tian, *Chem. Sci.*, 2018, **9**, 5709.
9 W. Ki and J. Li, *J. Am. Chem. Soc.*, 2008, **130**, 8114.
10 (*a*) D. F. Li, W. D. Hu, J. Wang, Q. W. Zhang, X. M. Cao, X. Ma and H. Tian, *Chem. Sci.*, 2018, **9**, 5709; (*b*) H. T. Z. Zhu, L. Q. Shangguan, D. Y. Xia, J. H. Mondal and B. B. Shi, *Nanoscale*, 2017, **9**, 8913; (*c*) Y. Z. Liu, L. Q. Shangguan, H. Wang, D. Y. Xia and B. B. Shi, *Polym. Chem.*, 2017, **8**, 3783; (*d*) L. Q. Shangguan, H. Xing, J. H. Mondala and B. B. Shi, *Chem. Commun.*, 2017, **53**, 889.
11 Y. H. Wen, T. L. Sheng, X. Q. Zhu, C. Zhuo, S. D. Su, H. R. Li, S. M. Hu, Q. L. Zhu and X. T. Wu, *Adv. Mater.*, 2017, **29**, 1700778.
12 (*a*) J. A. Li, J. H. Zhou, Z. Mao, Z. L. Xie, Z. Yang, B. J. Xu, C. Liu, X. Chen, D. Y. Ren, H. Pan, G. Shi, Y. Zhang and

Z. G. Chi, *Angew. Chem., Int. Ed.*, 2018, **57**, 6449; (*b*) Z. L. Xie, C. J. Chen, S. D. Xu, J. Li, Y. Zhang, S. W. Liu, J. R. Xu and Z. G. Chi, *Angew. Chem., Int. Ed.*, 2015, **54**, 7181.

13 (*a*) C. Rivas, G. J. Stasiuk, J. Gallo, F. Minuzzi, G. A. Rutter and N. J. Long, *Inorg. Chem.*, 2013, **52**, 14284; (*b*) W. R. Algar, D. Wegner, A. L. Huston, J. B. Blanco-Canosa, M. H. Stewart, A. Armstrong, P. E. Dawson, N. Hildebrandt and I. L. Medintz, *J. Am. Chem. Soc.*, 2012, **134**, 1876.

14 (*a*) N. Du, J. Song, S. Li, Y. X. Chi, F. Y. Bai and Y. H. Xing, *ACS Appl. Mater. Interfaces*, 2016, **8**, 28718; (*b*) C. L. Liu, R. L. Zhang, C. S. Lin, L. P. Zhou, L. X. Cai, J. T. Kong, S. Q. Yang, K. L. Han and Q. F. Sun, *J. Am. Chem. Soc.*, 2017, **139**, 12474.

15 S. X. Shang, Z. G. Lin, A. X. Yin, S. Yang, Y. N. Chi, Y. Wang, J. Dong, B. Liu, N. Zhen, C. L. Hill and C. W. Hu, *Inorg. Chem.*, 2018, **57**, 8831.

16 (*a*) G. A. Sotiriou, M. Schneider and S. E. Pratsinis, *J. Phys. Chem. C*, 2011, **115**, 1084; (*b*) F. Meiser, C. Cortez and F. Caruso, *Angew. Chem., Int. Ed.*, 2004, **43**, 5954; (*c*) J. Liu, A. Stace-Naughton, X. Jiang and C. J. Brinker, *J. Am. Chem. Soc.*, 2009, **131**, 1354.

17 (*a*) Q. Lin, T. T. Lu, X. Zhu, T. B. Wei, H. Li and Y. M. Zhang, *Chem. Sci.*, 2016, **7**, 5341; (*b*) Q. Lin, K. P. Zhong, J. H. Zhu, L. Ding, J. X. Su, H. Yao, T. B. Wei and Y. M. Zhang, *Macromolecules*, 2017, **50**, 7863; (*c*) Q. Lin, T. T. Lu, X. Zhu, B. Sun, Q. P. Yang, T. B. Wei and Y. M. Zhang, *Chem. Commun.*, 2015, **51**, 1635; (*d*) L. Y. Wang, H. H. Li, J. C. Deng and D. R. Cao, *Curr. Org. Chem.*, 2013, **17**, 3078.

18 (*a*) J. F. Chen, Q. Lin, Y. M. Zhang, H. Yao and T. B. Wei, *Chem. Commun.*, 2017, **53**, 13296; (*b*) Q. Lin, Y. Q. Fan, P. P. Mao, L. Liu, J. Liu, Y. M. Zhang, H. Yao and T. B. Wei, *Chem. – Eur. J.*, 2018, **24**, 777; (*c*) Q. Lin, Y. Q. Fan, G. F. Gong, P. P. Mao, J. Wang, X. W. Guan, J. Liu, Y. M. Zhang, H. Yao and T. B. Wei, *ACS Sustainable Chem. Eng.*, 2018, **6**, 8775; (*d*) T. B. Wei, J. F. Chen, X. B. Cheng, H. Li, B. B. Han, Y. M. Zhang, H. Yao and Q. Lin, *Org. Chem. Front.*, 2017, **4**, 210.